Cell proteins bind to multiple sites within the 5' untranslated region of poliovirus RNA

(mobility shift/RNA footprinting/eukaryotic initiation factor 2α)

Rosa Maria del Angel*, Athanasios G. Papavassiliou†, Carlos Fernández-Tomás*, Saul J. Silverstein†, and Vincent R. Racaniello†‡

†Department of Microbiology, Columbia University, 701 West 168th Street, New York, NY 10032; and *Departmento de Genética y Biologia Molecular, Centro de Investigación y de Estudios Avanzados, Mexico City, Distrito Federal, Mexico

Communicated by Harold S. Ginsberg, July 31, 1989

ABSTRACT   The 5' noncoding region of poliovirus RNA contains sequences necessary for translation and replication. These functions are probably carried out by recognition of poliovirus RNA by cellular and/or viral proteins. Using a mobility-shift electrophoresis assay and 1,10-phenanthroline/Cu⁺ footprinting, we demonstrate specific binding of cytoplasmic factors with a sequence from nucleotides 510–629 within the 5' untranslated region (UTR). Complex formation was also observed with a second sequence (nucleotides 97–182) within the 5' UTR. These two regions of the 5' UTR appear to be recognized by distinct cell factors as determined by competition analysis and the effects of ionic strength on complex formation. However, both complexes contain eukaryotic initiation factor 2α, as revealed by their reaction with specific antibody.

Poliovirus, a member of the Picornavirus family, contains a single-stranded RNA genome of positive polarity. This 7.5-kilobase RNA includes 5' and 3' untranslated regions (UTRs) of 745 and 73 nucleotides, respectively, whose functions are beginning to be revealed (reviewed in ref. 1). Analysis of the 5' UTR by site-directed mutagenesis indicates that it plays an important role in RNA replication and translation. For example, recently it was shown that ribosomes bind internally to sequences within the 5' UTR (2). Viral mutants with alterations in this region have been isolated that are defective in virus RNA replication (3, 4). This complex region also contains major determinants that attenuate neurovirulence (5–7). These functions are likely to be mediated by the interaction of cellular polypeptides with the 5' UTR.

To determine whether cell and/or viral polypeptides interact with the poliovirus 5' UTR, a mobility-shift assay was used to examine cytoplasmic extracts for their ability to form complexes with defined regions of the RNA. These studies reveal specific binding of cell factors with two sequences within the 5' UTR. One of these regions of binding was more precisely mapped by footprinting with a chemical nuclease. The translation initiation factor eIF-2α (eukaryotic initiation factor 2α) participates in complex formation with either sequence. However, competition analysis and determination of salt requirements for assembly of the complexes suggest that unique cellular factors are present in each complex. These RNA–protein interactions probably represent the initial steps in poliovirus replication.

MATERIALS AND METHODS

Cells, Viruses, and Recombinant DNAs. HeLa S3 cells were maintained as monolayers in Dulbecco's minimal essential medium containing 10% (vol/vol) horse serum as described

(8). For preparation of infected cell extracts, HeLa cells were infected at a multiplicity of infection of 100 with the P1/Mahoney strain of poliovirus. Poliovirus type 2 (P2/Lansing) cDNAs used for in vitro RNA synthesis (Fig. 1) have been described (9).

Preparation of Extracts. Confluent monolayers of mock-infected or poliovirus-infected cells 1–3 hr postinfection were scraped into 100 mM NaCl/1 mM EDTA/10 mM Tris·HCl, pH 7.5, and centrifuged; the cell pellet was resuspended in 10 mM NaCl/10 mM Tris·HCl, pH 7.5, and frozen and thawed three times. The extract was centrifuged in a microcentrifuge for 5 min and the supernatant (S10) was brought to 5% (vol/vol) glycerol and frozen in aliquots at −70°C. The ribosomal salt wash (RSW) was prepared as described (10).

Mobility-Shift Analysis. Labeled RNAs were prepared by in vitro transcription of cloned P2/Lansing cDNA templates with SP6 RNA polymerase and [α-³²P]UTP as described (9). Transcription reaction mixtures were then treated with RNase-free DNAse in the presence of RNasin (Promega), and unincorporated nucleotides were removed by gel filtration. Binding reactions were performed in a vol of 10 μl containing 10 mM Hepes-KOH (pH 7.4), 0.1 mM EDTA, 2 mM dithiothreitol, 8 mM MgCl₂, 4 mM spermidine, 5 mM ATP, 10% (vol/vol) glycerol, 12.5 units of RNasin (Promega), 150 ng of poly(rA-rC)·poly(rA-rC), 4 μg of tRNA, and 4 μg of a HeLa cell S10 or RSW. Reaction mixtures were assembled at room temperature and preincubated for 15 min. Uniformly labeled RNA (2.5–5 ng) was added and the mixture was incubated for 15 min at room temperature. For competition experiments, unlabeled RNA was added to the reaction mixture prior to the addition of labeled probe. Samples were loaded on a 6% polyacrylamide (acrylamide/bisacrylamide, 80:1) gel prepared in 0.5× TBE buffer (1× TBE buffer = 90 mM Tris/64.6 mM boric acid/2.5 mM EDTA, pH 8.3) and electrophoresed at constant current (15–20 mA) for 4–6 hr. Gels were then dried and autoradiographed.

Footprint Analysis. Unlabeled RNAs were synthesized as described above and phosphorylated with [γ-³²P]ATP and T4 polynucleotide kinase (11). Binding reactions were scaled up 10-fold and fractionated by gel electrophoresis. The free and bound RNAs (in separate lanes) were digested in situ by the nuclease activity of the 1,10-phenanthroline–Cu⁺ complex by a modification of the procedure of Kuwabara and Sigman (12). Briefly, after electrophoresis the gel was incubated in 10 mM Tris·HCl (pH 7.0) and exposed to 1,10-phenanthroline/Cu⁺ for 18 min. Free and bound RNAs were eluted by electrotransfer to NA45 membrane (Schleicher & Schuell) and subjected to analysis on 6% sequencing gels (13).

Abbreviations: UTR, untranslated region; eIF-2α, eukaryotic initiation factor 2α; RSW, ribosomal salt wash; CAT, chloramphenicol acetyltransferase.
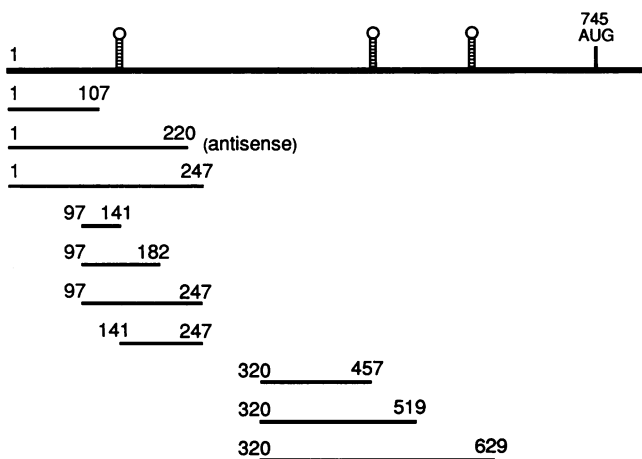‡To whom reprint requests should be addressed.

FIG. 1.   Locations of template RNAs containing various portions of the 5' UTR of poliovirus. The first 800 nucleotides of the viral RNA are shown at the top of the diagram as a thick line; the initiating AUG codon is indicated. Locations of three of the known and predicted stem and loop structures are depicted above the line. Boundaries of RNA transcripts used in the binding and competition assays are shown below the line. With the exception of the nucleotide 1–220 RNA, all others are plus stranded.

"Piggyback" Mobility Shifts. Complexes were formed with 4 μg of protein from a RSW fraction of HeLa cells. Antibodies (1 μg per μg of extract) were added after the second incubation and incubation was continued for an additional 40 min. Monoclonal antibody to eIF-2α was generously provided by E. Henshaw (14), and the monoclonal antibody to the herpes simplex virus gC glycoprotein was a gift from P. Spear (Northwestern University).

RESULTS

To determine whether specific regions of the poliovirus 5' UTR were recognized by cell proteins, ^{32}P-labeled RNAs were synthesized *in vitro* by using bacteriophage SP6 RNA polymerase from templates containing cloned regions of the 5' UTR (Fig. 1) and incubated with S10 extracts prepared from poliovirus-infected or mock-infected HeLa cells. Complex formation was monitored by electrophoresis through native polyacrylamide gels. Fig. 2*A* (lane 2) demonstrates that an RNA consisting of nucleotides 1–247 was recognized and bound by cell a factor(s) found in cytoplasmic extracts from mock-infected cells. Complexes identical in both abundance and electrophoretic mobility were detected when cytoplasmic extracts from virus-infected cells were used in the binding reaction (data not shown). The specificity of the complex that formed was demonstrated by competition experiments with homologous or heterologous unlabeled RNAs. The homologous RNA competed efficiently when present at only a 20-fold molar excess (lane 3), whereas a negative strand of nucleotides 1–220 from the 5' UTR (Fig. 1), or antisense transcripts of a bacterial chloramphenicol acetyltransferase (CAT) gene, were inefficient competitors, even at higher molar ratios of competitor to probe (Fig. 2*A*, lanes 6–11).

To further delineate sequences involved in complex formation, RNAs encompassing various portions of this region were synthesized and used as competitors in binding reactions with the nucleotide 1–247 RNA. Sequences from nucleotides 1–107, 97–141, and 141–247 did not inhibit complex formation when present at 20-fold molar excess (Fig. 2*B*, lanes 3–5). In contrast, an RNA from nucleotides 97–247 inhibited complex formation when present at a 20-fold molar excess (lane 6). Competition was also observed with an RNA
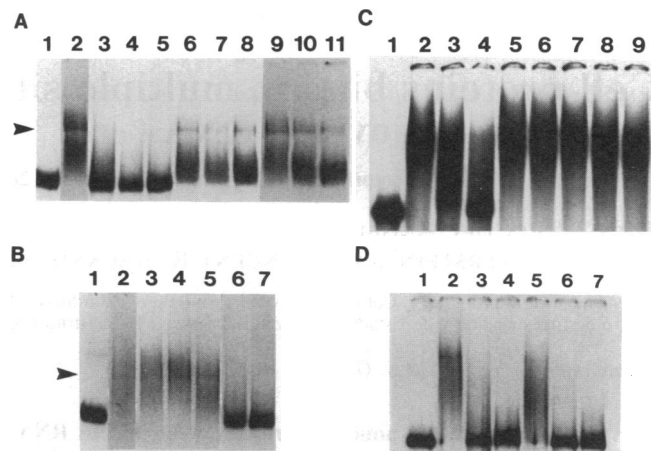
FIG. 2.   Mobility-shift analysis of RNAs from the poliovirus 5' UTR. (*A*) Binding and competition of the nucleotide 1–247 RNA. Labeled RNA was incubated with HeLa cell cytoplasmic extract in the presence of various molar equivalents of unlabeled competitor RNAs, and complex formation was assayed by mobility-shift analysis. Lanes: 1, probe incubated without extract; 2, probe with extract; 3–5, competition with, 20-, 50-, and 100-fold molar equivalents of the homologous unlabeled RNA, respectively; 6–8, competition with 20-, 50-, and 100-fold molar equivalents of unlabeled minus-stranded RNA (nucleotides 1–220) of the 5' UTR, respectively; 9–11, competition with 20-, 50-, and 100-fold molar equivalents of unlabeled antisense CAT RNA, respectively. (*B*) Nucleotide sequence requirements for complex formation with the nucleotide 1–247 RNA. Complex formation was carried out in the absence or presence of 20-fold molar equivalents of unlabeled RNAs from overlapping portions of the probe. Lanes: 1, probe incubated without extract; 2, probe incubated with extract; 3, competition with nucleotide 1–107 RNA; 4, competition with nucleotide 97–141 RNA; 5, competition with nucleotide 141–247 RNA; 6, competition with nucleotide 97–247 RNA; 7, competition with nucleotide 97–182 RNA. (*C*) Binding and competition of the nucleotide 320–629 RNA. Labeled RNA was incubated with HeLa cell cytoplasmic extract in the presence of various molar equivalents of unlabeled competitor RNAs, and complex formation was assayed by mobility-shift analysis. Lanes: 1, probe incubated without extract; 2, probe with extract; 3 and 4, competition with 10- and 20-fold molar equivalents of the homologous unlabeled RNA; 5, competition with 20-fold molar equivalents of nucleotide 1–247 RNA; 6, competition with 20-fold molar equivalents of nucleotide 320–457 RNA; 7, competition with 20-fold molar equivalents of nucleotide 320–519 RNA; 8, competition with 50-fold molar equivalents of minus-strand RNA (nucleotides 1–220) from the 5' UTR; 9, competition with 50-fold molar equivalents of antisense CAT RNA. (*D*) Binding and competition of the minus-stranded RNA (nucleotides 1–220) from the 5' UTR. Complex formation was performed in the absence or presence of 20-fold molar equivalents of unlabeled competitor RNAs. Lanes: 1, probe without extract; 2, probe with extract from mock-infected cells; 3 and 6, competition with homologous unlabeled RNA; 4, competition with unlabeled antisense CAT RNA; 5, probe with extracts from 1-hr poliovirus-infected cells; 7, competition with unlabeled antisense CAT RNA.

from nucleotides 97–182 (lane 7), further delimiting the sequences involved in complex formation. This RNA was also recognized and bound by a cell factor(s) found in S10 extracts (data not shown). These results demonstrate that the band detected by the mobility-shift assay represents specific complexes formed between a region of the viral genome from nucleotides 97–182 and constituents of the cytoplasm found in both mock- and virus-infected HeLa cells.

Complex formation was also observed with another region of the 5' UTR spanning nucleotides 320–629 and S10 extracts from mock-infected (Fig. 2*C*, lane 2) and virus-infected HeLa cells (data not shown). This interaction was specific because incubation with a 20-fold molar excess of the homologous fragment prevented the formation of stable complexes (lane

4). Moreover, complex formation was unaffected by a 50-fold molar excess of unlabeled RNAs from the minus strand (nucleotides 1–220 of the 5' UTR; Fig. 1), or antisense CAT gene transcripts (Fig. 2C, lanes 8 and 9). In addition, unlabeled RNAs encompassing nucleotides 1–247, 320–457, and 320–519 from the 5' UTR did not complete for binding when present at a 20-fold molar excess over the labeled probe (lanes 5–7). These results provide evidence that complex formation with this probe is limited to a region encompassing nucleotides 519–629 of the 5' UTR.

These experiments suggest that the nucleotide 97–247 and 320–629 RNAs both form unique complexes with different components of the cell cytoplasm. Alternatively, it is conceivable that the two RNAs are recognized by the same factors, but with different association or dissociation constants. Although the probes were of the same specific activity, the intensity of the band representing the complexes formed with the probe from nucleotides 1–247 was always less than that formed with the probe from nucleotides 320–629 (compare Fig. 2A, lane 2, and Fig. 2C, lane 2). We have not yet investigated the basis for this difference.

To demonstrate the specificity and fidelity of these reactions, we examined the binding properties of an RNA derived from the minus strand of nucleotides 1–220 from the 5' UTR by the mobility-shift assay. Although this RNA formed complexes with mock- and virus-infected extracts (Fig. 2D, lanes 2 and 5), binding was effectively blocked by competition with a 20-fold molar excess of either homologous (lanes 3 and 4) or heterologous (lanes 6 and 7) unlabeled RNAs. These results demonstrate that nonspecific and specific binding are easily distinguished.

No difference in the amounts and electrophoretic mobilities of the complexes formed with either nucleotide 1–247 or 320–629 probes was observed when S10 extracts from either mock-infected or infected HeLa cells were used. However, when the salt requirements for assembly of the complexes were assessed by incubation with increasing amounts of KCl, the probes behaved differently. Complex formation with the nucleotide 1–247 RNA was detected up to 120 mM KCl in mock-infected cell extracts but was abolished when the same concentration of KCl was used in binding reactions done with infected cell extracts (Fig. 3A). In contrast, the complex formed with the nucleotide 320–629 RNA in mock-infected cell extracts at 120 mM KCl migrated faster than those formed at lower concentrations of KCl or in infected cell extracts regardless of salt concentration (Fig. 3B). These results emphasize the distinct nature of the complexes formed with these two regions of the 5' UTR.

To more precisely map binding sites within each probe, we adapted the chemical nuclease cleavage procedure of Kuwabara and Sigman for footprinting DNA–protein complexes (12). In this procedure, separation of complexed and free probe is followed by treatment of the gel with the 1,10-phenanthroline/Cu$^+$ reagent, resulting in cleavage of accessible phosphodiester bonds in DNA. As with conventional footprinting techniques, 1,10-phenanthroline/Cu$^+$ protection identifies sequences protected from cleavage by the nuclease. Accordingly, each RNA probe was incubated in the presence or absence of cytoplasmic extract, under conditions in which all of the RNA probe was bound. The free and bound samples were then fractionated by gel electrophoresis, and the gel was exposed to the 1,10-phenanthroline/Cu$^+$ reagent *in situ*. The RNAs were eluted from the gel and analyzed by electrophoresis in a denaturing polyacrylamide gel.

The electrophoretic pattern of the RNA derived from the nucleotide 320–629 complex revealed a protected region toward the 3' end of the sequence (Fig. 4B). The markers permitted assignment of the 5' boundary of this region to approximately nucleotide 550, while the 3' boundary maps very close to nucleotide 629 (Fig. 4C). In addition, increased
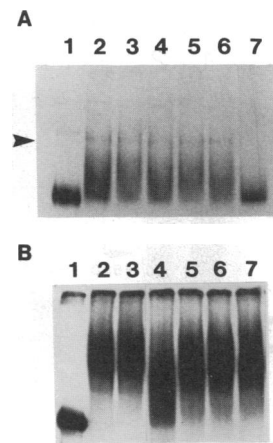

FIG. 3.　Effect of KCl on binding in mock-infected and poliovirus-infected HeLa cell cytoplasmic extracts. (A) The nucleotide 1–247 RNA probe (lane 1) was incubated with S10 extracts from mock-infected (lanes 2–4) or poliovirus-infected (lanes 5–7) cells, in the presence of 5 mM (contributed by the extract; lanes 2 and 5), 60 mM (lanes 3 and 6), or 120 mM (lanes 4 and 7) KCl. Complex formation was monitored by mobility-shift assay. (B) The nucleotide 320–629 RNA probe (lane 1) was incubated with S10 extracts from mock-infected (lanes 2–4) or poliovirus-infected (lanes 5–7) cells in the presence of 5 mM (lanes 2 and 5), 60 mM (lanes 3 and 6), or 120 mM (lanes 4 and 7) KCl. Complex formation was monitored by mobility-shift assay. Arrowhead indicates the complex formed with the nucleotide 1–247 RNA.

cleavages were observed in the region upstream of nucleotide 500 (arrowheads in Fig. 4B). These are probably enhanced cleavage and not overdigestion of the RNAs, because identical amounts of RNA (cpm) were present in the lanes containing bound and free RNA, and these samples were treated with 1,10-phenanthroline/Cu$^+$ *in situ* under identical conditions. Furthermore, increased cleavage was not observed at all possible sites, as would be expected if the RNAs were overdigested. The 1,10-phenanthroline/Cu$^+$ reagent preferentially attacks double-stranded regions of nucleic acids (16); nucleotides 451–559 form a highly ordered and evolutionarily conserved secondary structure as revealed by dimethyl sulfate protection and nuclease sensitivity studies (17, 18). Enhanced scission of nucleic acids is thought to result from increased accessibility of specific nucleotide sequences to cleavage. Increased accessibility may in turn result from a conformational change induced by binding of a protein(s) adjacent to the putative stem and loop structure.

A similar analysis performed with the nucleotide 97–182 complex demonstrated that no sequences were protected from chemical cleavage (Fig. 4A). However, the area between nucleotides 120 and 160 displayed enhanced cleavages (arrowheads in Fig. 4A). Computer analysis predicts a stable stem and loop structure in this region that is conserved among picornaviruses (18, 19).

It was of interest to determine whether the complexes formed with these areas of the 5' UTR contain translation factors, because the region between nucleotides 140 and 630 acts as an entry point for ribosomes, leading to internal initiation of translation (2). Therefore, a RSW was prepared and incubated with each probe. Mixtures analyzed by the mobility-shift assay demonstrated that both the nucleotide 1–247 and 320–629 probes formed specific complexes (Fig. 5A). These complexes comigrated with those formed with cytoplasmic extracts (Fig. 5B for the nucleotide 320–629 RNA; data not shown for the nucleotide 1–247 RNA). The absence of complex formation when the minus-strand RNA probe (nucleotides 1–220) was incubated in the RSW (Fig. 5A, lane 1) demonstrated the specificity of these interactions.
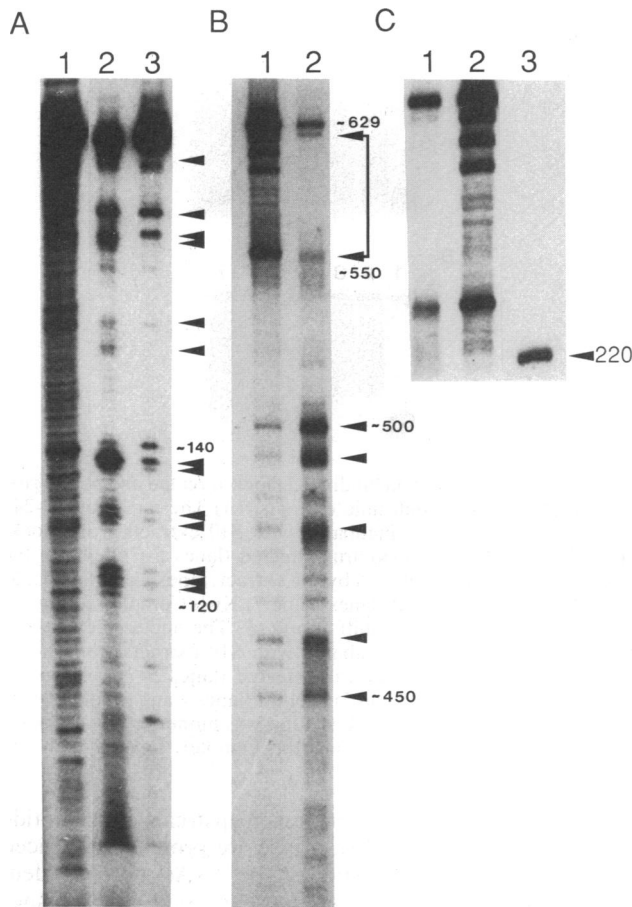
FIG. 4. Footprinting analysis. Free and bound RNAs were subjected to chemical cleavage *in situ* with 1,10-phenanthroline/Cu^+, eluted from the gel, and analyzed by electrophoresis on denaturing polyacrylamide gels. (*A*) Analysis of bound (lane 2) and free (lane 3) nucleotide 1–247 RNAs. Lane 1, probe subjected to partial alkaline hydrolysis (15). (*B*) Analysis of free (lane 1) and bound (lane 2) nucleotide 320–629 RNAs. (*C*) Analysis of bound (lane 1) and free (lane 2) nucleotide 320–629 RNAs after longer electrophoresis. Lane 3 contains a 220-nucleotide RNA size marker; the upper band in lanes 1 and 2 is the 309-nucleotide probe. Arrowheads indicate bands whose intensities are enhanced after chemical cleavage of the bound RNA fraction. Approximate nucleotide positions (1 is the first nucleotide of the viral genome) are shown next to arrowheads for *A* and *B*. Line in *B* indicates the protected region (nucleotides 550–629).

To determine whether known translation factors of the RSW were involved in complex formation, a monoclonal antibody to eIF-2α was added either before or after incubation of each probe with the RSW, and the reaction mixtures were analyzed by gel electrophoresis. Migration of the complexes formed with the nucleotide 320–629 and 1–247 probes was dramatically reduced if antibody was added either before or after incubation with the RSW (Fig. 5*A*). Identical results were obtained when the two probes were incubated with cytoplasmic extract (data not shown). Control reactions containing bovine serum albumin or monoclonal antibodies specific for several herpes simplex virus proteins had no effect on the mobility of the complexes formed (Fig. 5*A*). Apparently eIF-2α is a component of the complexes formed when these probes are incubated with cytoplasmic extracts. Because preincubation of the extract with the antibody had no effect on binding, it is clear that the monoclonal antibody recognizes an epitope that is not involved in complex formation with either the nucleotide 1–247 or 320–629 sequence.

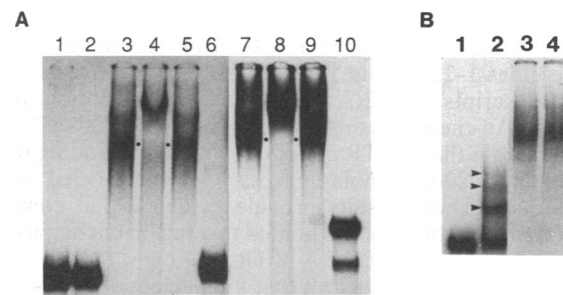To examine the participants in the generation of these complexes, the nucleotide 320–629 RNA was incubated with

FIG. 5. Complexes formed with RSW. (*A*) Identification of eIF-2α in the complexes. RNAs of nucleotides 1–220 (antisense, lanes 1 and 2), 1–247 (lanes 3–6), and 320–629 (lanes 7–10) were incubated alone (lanes 2, 6, and 10), with the RSW (lanes 1, 3–5, and 7–9), with a control antibody (lanes 3 and 7), or with antibody specific for eIF-2α (lanes 4 and 8), prior to mobility-shift analysis. (*B*) Effect of RSW concentration. RNA nucleotides 320–629 was incubated alone (lane 1), with 0.4 μg (lane 2), or 4 μg (lane 3) of RSW prepared from mock-infected HeLa cells, or with 4 μg of S10 extract, and analyzed by mobility-shift assay. Arrowheads indicate the multiple complexes observed at low concentrations of RSW.

two different concentrations of RSW (Fig. 5*B*). When the lower concentration (0.4 μg) was used, three distinct complexes were detected (lane 2). These could result from binding of a factor(s) to several sites within the RNA or from interactions between RNA binding and non-RNA binding proteins. At the higher concentration (4 μg), only a single slower migrating complex formed (lane 3). The abundance and electrophoretic mobility of this complex were indistinguishable from the complex formed with this probe and the S10 fraction (lane 4). Thus, formation of this complex is a multistep process involving more than one protein, which is facilitated by cooperative interactions between cellular factors.

DISCUSSION

The experiments described here demonstrate that at least two regions of the 5' UTR of the poliovirus genome specifically interact with components of the cell cytoplasm. The complexes formed can be distinguished by competition analysis and their sensitivity to KCl. However, both complexes contain eIF-2α. Because ribosomes are known to bind and initiate translation internally on the poliovirus genome (2), it is perhaps not surprising that eIF-2α is found in complexes that map to regions within the 5' UTR.

The formation of the complex between cytoplasmic proteins and the nucleotide 320–629 RNA is sensitive to 120 mM KCl in mock-infected extracts, while a more rapidly migrating complex is detected at this ionic strength in infected cell extracts. The basis for the altered mobility is not known, but it may be a consequence of phosphorylation of eIF-2α that occurs after poliovirus infection (24).

The binding and competition experiments were designed to delimit the sequences within the 5' UTR recognized and bound by cell factors. One region identified by these analyses consists of nucleotides 97–182. It is predicted to contain a stem and loop structure from nucleotides 125–164 (19). Only an RNA containing at least nucleotides 97–182, which includes the putative stem and loop, competes with nucleotides 1–247 for binding. RNAs lacking the complete stem and loop structure do not compete, suggesting that its integrity is important for binding. To further define these interactions, 1,10-phenanthroline/Cu^+ cleavage was used to identify sequences that were either protected from or more exposed to chemical cleavage. Although areas of the nucleotide 1–247 probe were not protected from cleavage with the 1,10-phenanthroline/Cu^+ reagent, the region containing the pu-

tative stem and loop shows an enhanced cleavage pattern after treatment with this reagent.

Competition experiments defined the region of binding for the nucleotide 320–629 RNA between 510 and 629. 1,10-Phenanthroline/Cu$^+$ footprinting identified a protected region within this sequence between nucleotides 550 and 629. This region contains a thermodynamically stable stem and loop structure (nucleotides 585–620) with an extended perfect duplex (nucleotides 582–620) that is conserved among different picornaviruses (18, 19). The stem and loop is part of a larger domain (nucleotides 140–631) required for internal initiation of translation of poliovirus RNA both *in vitro* and *in vivo* (2, 20). Mutation of an A to a U at nucleotide 588, within the nucleotide 582–620 duplex, resulted in a small plaque variant with reduced translational efficiency (21). Deletion of nucleotides 600–729 has no effect on virus growth, while deletion of nucleotides 556–729 results in a small plaque phenotype, and infectivity is lost when nucleotides 551–729 are deleted (22). Finally, it was reported that a 60-nucleotide sequence from nucleotides 567–627 is important for efficient translation *in vitro* (23). Thus, a region required for efficient translation of viral RNA maps between nucleotides 556 and 600. This region, identified by genetic analyses, overlaps with the sequences protected from chemical cleavage. In addition to the protected region, areas of enhanced cleavage were detected upstream of this sequence. These enhancements map to a region of known secondary structure as defined by chemical and enzymatic probing (17, 18) and may result from increased accessibility induced by protein binding in the downstream region.

What is the role of the complexes that include eIF-2α? We speculate that, because eIF-2α is part of the translation initiation machinery, these interactions may represent an early step in virus replication that precedes ribosome binding to poliovirus mRNA. This notion is supported by the genetic studies discussed above, as well as by the observation that the 5′ UTR of poliovirus RNA contains an internal entry site for ribosome binding (2).

Whether eIF-2α recognizes RNA binding proteins, specific features of a primary sequence domain or secondary structure remain to be determined. The contribution of primary and secondary structure to the formation of these complexes will require further analysis by mutagenesis. It will also be necessary to identify other components of these complexes and to determine whether other regions of the 5′ UTR are recognized by cell proteins. A combination of mutagenesis, mobility-shift analysis, and studies of viral RNA synthesis and translation is required to elucidate the functional significance of the RNA–protein interactions that we have identified.

1. Wimmer, E., Kuhn, R., Pincus, S., Yang, C., Toyoda, H., Nicklin, M. & Takeda, N. (1987) in *Virus Replication and Genome Interaction: Seventh John Innes Symposium*, ed. Davies, J. W. (Company of Biologists, Cambridge, England), Vol. 7, pp. 251–276.
2. Pelletier, J. & Sonenberg, N. (1988) *Nature (London)* **334**, 320–325.
3. Trono, D., Andino, R. & Baltimore, D. (1988) *J. Virol.* **62**, 2291–2299.
4. Racaniello, V. R. & Meriam, C. (1986) *Virology* **15**, 498–507.
5. Kawamura, N., Kohara, M., Abe, S., Komatsu, T., Tago, K., Arita, M. & Nomoto, A. (1989) *J. Virol.* **63**, 1302–1309.
6. Westrop, G. D., Wareham, K. A., Evans, D. M. A., Dunn, G., Minor, P. D., Magrath, D. I., Taffs, F., Marsden, S., Skinner, M. A., Schild, G. C. & Almond, J. W. (1989) *J. Virol.* **63**, 1338–1344.
7. Moss, E. G., O'Neill, R. E. & Racaniello, V. R. (1989) *J. Virol.* **63**, 1884–1890.
8. La Monica, N., Meriam, C. & Racaniello, V. R. (1986) *J. Virol.* **57**, 515–525.
9. Pelletier, J., Kaplan, G., Racaniello, V. & Sonenberg, N. (1988) *Mol. Cell Biol.* **8**, 1103–1112.
10. Dasgupta, A., Zabel, P. & Baltimore, D. (1980) *Cell* **19**, 423–429.
11. Maniatis, T., Fritsch, E. & Sambrook, J. (1982) *Molecular Cloning: A Laboratory Manual* (Cold Spring Harbor Lab., Cold Spring Harbor, NY).
12. Kuwabara, M. D. & Sigman, D. S. (1987) *Biochemistry* **26**, 7234–7238.
13. Sanger, F., Nicklen, S. & Coulson, A. (1977) *Proc. Natl. Acad. Sci. USA* **74**, 5463–5467.
14. Scorsone, K. A., Panniers, R., Rowlands, A. G. & Henshaw, E. C. (1987) *J. Biol. Chem.* **2**, 14538–14543.
15. Donis-Keller, H., Maxam, A. M. & Gilbert, W. (1977) *Nucleic Acids Res.* **4**, 2527–2538.
16. Marshall, L. E., Graham, D. R., Reich, K. A. & Sigman, D. S. (1981) *Biochemistry* **20**, 244–250.
17. Skinner, M. A., Racaniello, V. R., Dunn, G., Cooper, J., Minor, P. D. & Almond, J. W. (1989) *J. Mol. Biol.* **207**, 379–392.
18. Pilipenko, E. V., Blinov, V. M., Romanova, L. I., Sinyakov, A. N., Maslova, S. V. & Agol, V. I. (1989) *Virology* **168**, 201–209.
19. Rivera, V., Welsh, J. & Maizel, J. J. (1988) *Virology* **165**, 42–50.
20. Pelletier, J. & Sonenberg, N. (1989) *J. Virol.* **63**, 441–444.
21. Pelletier, J., Flynn, M. E., Kaplan, G., Racaniello, V. & Sonenberg, N. (1988) *J. Virol.* **62**, 4486–4492.
22. Kuge, S. & Nomoto, A. (1987) *J. Virol.* **61**, 1478–1487.
23. Bienkowska-Szewczyk, K. & Ehrenfeld, E. (1988) *J. Virol.* **62**, 3068–3072.
24. O'Neill, R. & Racaniello, V. R. (1989) *J. Virol.*, in press.